ANALYSIS OF SPATIAL DISTRIBUTION IN TROPOSPHERIC AND SEA SURFACE TEMPERATURE TRENDS

A Thesis
Presented to
The Academic Faculty

by

Paula A. Agudelo

In Partial Fulfillment
of the Requirements for the Degree
Master of Sciences in the
School of Earth and Atmospheric Sciences.

School of Earth and Atmospheric Sciences
Georgia Institute of Technology
April 2005

ANALYSIS OF SPATIAL DISTRIBUTION IN TROPOSPHERIC AND SEA SURFACE TEMPERATURE TRENDS

Approved by:

Dr. Judith A. Curry, Advisor
School of Earth and Atmospheric Sciences
Georgia Institute of Technology

Dr. Robert Dickinson
School of Earth and Atmospheric Sciences
Georgia Institute of Technology

Dr. Peter J. Webster
School of Earth and Atmospheric Sciences
Georgia Institute of Technology

Date Approved: April 11 2005

To Carlos,

His help and patience has allowed me accomplish my goals. I can only hope that throughout our life time together, I can find ways to repay him.

ACKNOWLEDGEMENTS

I would like to acknowledge the people that have contributed to this work. I specially thank my advisor, Dr. Judith Curry, for providing me support and guidance. I would like to thank my committee members Drs. Robert Dickinson and Peter Webster for their time and useful comments.

Additionally, I would like to thank my parents who laid the foundation by teaching me the principles, values and hard work discipline that have served me well in all aspects of life. Also to my brothers and uncle for being available for every crazy thing that I needed. Although they still don't know what I am doing, they love me enough to feign excitement anyway.

Especially I want to thank Carlos for stood by my side in every moment and do not let me go the easiest way of quit and go home.

TABLE OF CONTENTS

LIST OF TABLES

LIST OF FIGURES

SUMMARY

Regional patterns in tropospheric and sea surface temperature (SST) trends are examined for the period 1979-2001 using MSU, NCEP-NCAR, ECMWF ERA-40 reanalyses, NOAA OI SST, and the CARDS radiosonde data set. Trends are estimated using a nonparametric Mann-Kendall approach. Substantial regional variability in temperature trends is seen in all of these data sets, with the magnitude of the variability (including substantial regions with cooling trends) far exceeding the average warming trend. The global analyses from MSU and the NCAR/NCEP and ECMWF reanalyses are used to identify sampling problems in using the radiosonde network to infer global trends. Analysis of the trends in tropospheric temperature concurrent with the trends in sea surface temperature shows regions where the signs disagree for both surface cooling and warming. Interpretation of these differing trends using the reanalyses suggest that the models used for the reanalyses are simulating the necessary dynamics/thermodynamics that could lead to a tropospheric cooling in contrast to a surface warming (and vice versa).

CHAPTER I

INTRODUCTION

The impacts of human activities on the global climate have been of great concern since the last century. Scientific research has indicated that human activities are changing atmospheric composition in ways that are very likely to cause significant global warming.

Documenting trends in atmospheric temperature is a key factor to understanding climate change and evaluating model simulations of this change (e.g. NRC 2000, Houghton et al. 2001). Considerable efforts have been made to determine atmospheric temperature trends from radiosonde observations and also from satellites (e.g. Angell 1988, 2003, Hurrell et al. 2000, Gaffen et al. 2000, Lanzante et al. 2003b, Santer et al. 2000, Seidel et al. 2004). Different analyses have produced diverse results, including apparent inconsistencies of tropospheric temperature trends with trends in surface temperature.

The types of observational data available for an investigation on temperature trends are diverse. They differ in the type of measurement, length of time period, and space-time sampling. There have been several investigations of trends that have considered varying time spans with the different available data sets. Different groups have addressed data quality, spatial sampling, and temporal homogeneity issues differently, and no single data product has emerged as a generally recognized reference.

Angell (1988), using 63 radiosonde sites with data from 1958 to 1987, found a global increase of tropospheric temperature (850-300 mb) and temperature decrease in the tropopause (300-100 mb) as well as in the lower stratosphere (100-50 mb). Since the original analysis of atmospheric temperature trends by Angell (1988), numerous analyses have focused on obtaining homogeneous data sets, free of gradual and sudden artificial temperature changes resulting from observation procedures (e.g. Lanzante et al. 2003a, Prabhakara et al. 2000, Christy et al. 2003).

Santer (1999) dealt with general uncertainties associated with estimation of temperature changes in the free atmosphere by considering radiosonde, satellite and reanalysis data. Among the uncertainty sources when using radiosonde data is the inhomogeneous distribution across the earth's surface. Gaffen (1994), Gaffen et al. (2000), and Lanzante et al. (2003a) show that changes in radiosonde equipment and operational procedures, which are unique to each specific country, may introduce errors in trend estimation.

In particular, Lanzante et al. (2003a) developed a two-step subjective method to identify artificial discontinuities and adjust or discard the data. Another source of uncertainty is the different statistical methods used to estimate trends (e.g. Gaffen et al. 2000, Santer et al. 2000). A general conclusion has been that the estimation of global average trends from radiosonde data is robust in sign against uncertainties due to different data sets and statistical methods used. In particular, Lanzante et al. (2003a) conclude that artificial discontinuities in radiosonde data are not large enough to alter the average global atmospheric tendencies.

An implicit assumption in most analyses is that trends determined using the global radiosonde network (predominantly over Northern Hemisphere land locations) is sufficient to infer global atmospheric temperature trends. Satellites can provide global analyses of atmospheric temperature trends. Data from the Microwave Sounding Unit (MSU) on board the National Oceanic and Atmospheric Administration (NOAA) operational satellites, available since 1979, have been used in different temperature trend analyses (Christy et al 2003, Mears et al. 2003). Challenges when determining trends from satellite include calibration drift, temporal drift, and intercalibration among different satellites. These uncertainties, notably the manner in which NOAA-9 is calibrated, have resulted in different analyses of atmospheric temperature trends from the MSU data.

While most studies have focused on the analysis of average global or hemispheric trends in atmospheric temperature, the goal of this reaearch is to analyze the spatial distribution of recent trends in tropospheric and sea surface temperatures. To address this issue, we use diverse data sets and examine the most prominent regional features. No attempt here is made to establish definitive magnitudes in the trends; rather this work focuses on the regional variations in the trends and their consistency among the data sets. It is also argued that the use of average global trends can be misleading both in documenting and understanding the temperature trends, since the observed trends are not spatially homogeneous, with both warming and cooling trends apparent. Further, because of regional variability in the trends, inference of global trend from the radiosonde network can be misleading owing to sampling issues.

In order to address this issues, this document is organized as follows. Chapter 2 describes the radiosonde, satellite and reanalyses data sets used in the present work, as well as the statistical methodologies applied to estimate temperature trends. Chapter 3 presents the analysis of the spatial distribution in tropospheric and surface temperature trends using different data sets. Finally, conclusions are presented in Chapter 4.

CHAPTER II

DATA AND METHODOLOGY

Data sets used in this analysis include both satellite-based, and numerical weather prediction reanalysis products for the period 1979-2001. Additional global analyses are obtained from surface and radiosonde measurements. Satellite instruments that remotely sense tropospheric temperatures have become available since 1979. An important attribute of the satellites is their global coverage. The satellite instruments fall into two categories: remotely sensing in the microwave, and thermal infrared wavelengths. In contrast to the ground-based measurements, for example, the radiosonde, which perform measurements at specific pressure levels, the available satellite sensors sense the signal from a wide range in altitude.

One of satellite-based products used in the study is the latest version (5.1) of the University of Alabama in Huntsville (UAH) MSU retrieval dataset. Microwave sounding units (MSUs) on NOAA polar-orbiting satellites have monitored the intensity of radiation from (primarily) atmospheric oxygen since the first satellite was launched in December 1978. The magnitude of this intensity is proportional to air temperature. The overall stability of the instruments and the robustness of the measurements have provided a way to create relatively long time series of bulk temperatures for atmospheric layers several kilometers deep.

Version 5.1 is the result of minor modifications made to version 5.0 described in

Christy et al (2003). Some of these changes include, for example, the strengthening of the requirement for acceptable data to enter into the routine that calculates the intersatellite biases. The MSU product are the TLT and the TMT (formerly known as T2LT and T2) that represent the low-middle troposphere and the midtroposphere repectively. The spatial resolution is 2.5 degrees. 90% of the emissions originate below 400 hPa for the MSU TLT and below 120 hPa for MSU TMT.

Another satellite-based product, the NOAA Optimum Interpolation (OI) Sea Surface Temperature (SST) based on the V2 data, was used to calculate tendencies for this variable (Reynolds and Smith, 1994). This dataset consist in monthly fields with a spatial resolution of one-degree grid. A new version of the Global sea-Ice and Sea Surface Temperature dataset (GISST Version 2.3b) that updates GISST 2.2 and is describe by Rayner et al. (1996) was also considered. GISST provides one-degree monthly SST for 1871 to February 2003. GISST data set was put together by the Hadley Centre of the UK Meteorological Office. HadCRUT2, a combined land and marine temperature anomalies dataset on a 5-degree grid produced by the Climatic Research Unit of the University of East Anglia (UK) was also used (Rayner et al. 2003).

This work includes analysis of data from the Television Infrared Observation Satellite (TIROS) Operational Vertical Sounder (TOVS) system, flown on the NOAA Operational Polar Orbiting Satellite series, obtained from the International Satellite Cloud Climatology Project (ISCCP) data set. This product has a spatial resolution of 280 km equal-area global grid, a daily temporal resolution, and it is available for 9

different levels (900, 740, 620, 500, 375, 245, 115, 50, and 15mb). Data are available from 1983 to 2001 (Rossow et al. 1996).

Global temperature anomalies based on 87 homogenized radiosonde stations part of the Comprehensive Aerological Reference Data Set (CARDS) (Eskridge et al. 1995, Lanzante et al. 2003a, Seidel et al 2004) were utilized in this work. While there are more stations available, the record of these 87 stations has been carefully analyzed and corrected for missing data and artificial trends due to changes in the measurement equipment. CARDS data is based on daily (up to four per day) radiosonde observations collected from over 20 data sources and range from 1940 to 2000. The spatial distribution of 155 CARDS stations part of GUAN (GCOS -Global Climate Observing System- Upper air network) is also used.

Tropospheric temperatures from two reanalyses, National Center for Environmental Prediction - National Center for Atmospheric Research (NCEP-NCAR) described in Kalnay et al. (1996) and European Centre for Medium-Range Weather Forecasts (ECMWF) ERA-40 described in Simmons and Gibson (2000) are also evaluated. The ECMWF and NCEP-NCAR reanalyses are included here as additional sources of information on regional variability in atmospheric temperature trends. While the utility of the reanalyses have not been established for determining the magnitude of the temperature trends, the regional variability of the trends are considered here to supplement the MSU analysis.

NCEP Reanalysis data and NOAA Optimum Interpolation (OI) SST V2 data was provided by the NOAA-CIRES Climate Diagnostics Center, Boulder, Colorado,

USA, from their Web site at www.cdc.noaa.gov. Christy et al. MSU data set was obtain from www.ghcc.msfc.nasa.gov, ECMWF ERA- 40 data have been obtained from the ECMWF data server at data.ecmwf.int/data/, and HadCRUT2 data was obtained from www.cru.uea.ac.uk/cru/data/temperature/.

To compute temperature trends, monthly anomalies were generated as deviations from the mean monthly values over the data period for each data set. MSU and HadCRUT2 data are made available as monthly anomalies by their respective authors.

There is a wide range in the numerical methods reported in the literature to derive trends and their significance. Most studies are based on linear regression analyses, although details of the mathematical models and particularly aspects of the standard error estimates vary. Differences in details of the models include the method of fitting seasonal variability, the number and types of proxies included for atmospheric dynamics, and the method used to account for serial autocorrelation of meteorological variables.

Some recent studies (e.g. Santer et al. 2000, Gaffen et al. 2000) have examined trend uncertainties in layer-average free atmosphere temperatures arising from the use of different trend estimation methods, suggesting the sensitivity of linear trends to the choice of fitting method. Such studies have also rise the issue relative to the significance of trends and the question of which procedures one might use in order to determine significance. In order to cover this concern this study includes a nonparametric method to test for the existence of trend and three different methods for the estimation of these trends.

Testing for trends was conducted, as mention before, using the nonparametric Mann-Kendall test (Mann 1945, Kendall 1938), and variations of it that consider seasonality and serial correlation, which are commonly used for atmospheric and hydrologic data analysis (e.g., Hirsch et al. 1982, Molnar and Ramirez 2001). An advantage of the nonparametric test is that no assumption of a specific distribution of the monthly anomalies of temperature is necessary. These rank-based procedures are suitable to detect monotonic trend, not necessarily linear, during some interval of time. According to Mann, the null hypothesis of randomness H_0 states that the data $(x_1, \ldots, x_n)$ are a sample of η independent and identically distributed random variables. The alternative hypothesis H_1 is that the distribution of x_k and x_j are not identical for all k, $j \leq n$ with $k \neq j$. The trend test statistic S (Kendall statistic) as defined by Hirsch et al. (1982) is

$$S = \sum_{k=1}^{n-1} \sum_{j=k+1}^{n} \operatorname{sgn}(x_j - x_k) \tag{1}$$

where

$$\operatorname{sgn}(\xi) = \begin{cases} 1 & \text{if} \quad \xi > 0 \\ 0 & \text{if} \quad \xi = 0 \\ -1 & \text{if} \quad \xi < 0 \end{cases} \tag{2}$$

The mean and variance of S under H_0 are given by

$$\mathrm{E}[S] = 0 \tag{3}$$

$$\mathrm{Var}[S] = \frac{n(n-1)(2n+5) - \sum_t t(t-1)(2t+5)}{18} \tag{4}$$

where t is the extent of any given tie and $\sum_t$ denotes the summation over all ties. Given that both Mann (1945) and Kendall (1938) showed that the normality approximation for S is excellent even for small n ($n \approx 10$), the standard normal variate Z used for hypothesis testing is

$$Z = \begin{cases} \frac{S-1}{\sqrt{(\mathrm{Var}(S))}} & \text{if} \quad S > 0 \\ 0 & \text{if} \quad S = 0 \\ \frac{S+1}{\sqrt{(\mathrm{Var}(S))}} & \text{if} \quad S < 0 \end{cases} \tag{5}$$

In a two-sided test for trend, H_0 is rejected at significance level α if $|Z| > z_{1-\frac{\alpha}{2}}$, where $\frac{\alpha}{2}$ is the value of the standard normal distribution with a probability of exceedance of $\frac{\alpha}{2}$. A positive value of Z indicates an upward trend and a Z negative indicates a downward trend.

We also used a *Seasonal Kendall* test for trend introduced by Hirsch et al. (1982). This procedures account for the existence of seasonality. Seasonality is partially removed from the data described before (monthly anomalies) by the removal of the annual cycle, but since we did not modified the anomalies to account for the different monthly variances, the seasonal Kendall trend tests is relevant in our calculations. To

perform the seasonal test, the data is classified by month of the year and the Kendall statistic is quantified as explained before but for each month separately, so there are twelve different values of S_i, where i represents each month. Then, $S' = \sum_{i=1}^{12} S_i$ is defined. From Hirsch et al. (1982), the expected value and variance of S' are defined as

$$\mathrm{E}\left[S'\right] = 0 \tag{6}$$

$$\mathrm{Var}\left[S'\right] = \sum_{i=1}^{12} \mathrm{Var}\left[S_i\right] + \sum_{i=1}^{12}\sum_{l=1}^{12} \mathrm{cov}\left[S_i S_l\right] \tag{7}$$

In this approach, under H_0, S_i and S_l with $i \neq l$, are assumed functions of independent random variables so $\mathrm{cov}\left[S_i S_l\right] = 0$. Knowing that, Z is finally computed as in the original Kendall test.

Since the main purpose is to quantify the temperature trends as a slope, i.e. change per unit time, not necessarily implying that in this specific case the trend has to be linear, it is possible to use the seasonal Kendall slope estimator B as defined by Hirsch et al. (1982). First, the index d_{ijk} is computed as $d_{ijk} = \frac{(x_{ij} - x_{ik})}{j-k}$ for all (x_{ij}, x_{ik}) pairs, with $i = 1, 2, \ldots, 12$, and $1 \leq k < j \leq n_i$, where $x_{\alpha\beta}$ is the temperature anomaly for month α and year β, and n_α is the number of data points available for month α. Then B is defined as the median of these d_{ijk} values, which makes it non-parametric and robust against the effect of extreme values.

We compared B with the slope estimated by linear regression using a least-squares estimator (LS) and a least absolute deviation estimator (LAD). The LS estimator

corresponds to the slope obtained with a linear-fitting method calculated with the traditional least squares approach that minimizes the mean square deviation between the data points and the trend line. Since in geophysics there is no a priori reason why a LS fit should be preferable to alternative linear-fitting methods, results were compared to trends obtained with a LAD estimator. LAD regression differs from LS regression in that the sum of the absolute, not squared, deviations of the fit from the observed values is minimized, thus is less sensitive to extreme values. Different studies have shown that over the relatively short records, the two methods of obtaining linear fits can yield large trend differences (e.g. Santer et al., 2000).

CHAPTER III

RESULTS

Figure 1 shows the spatial distribution of the seasonal Kendall statistic (Z) for UAH MSU TLT dataset. In this case negative values of Z indicate the existence of negative (cooling) trends while positive Z represent positive (warming) ones. Greater absolute values of Z indicate higher probability of rejecting the null hypothesis of randomness, implicating a more statistically significant trend irrespective of the sign. The area within the green line corresponds to the regions where randomness is rejected at 95% significance level or higher. Estimation of the temperature trends in °C/Decade for the UAH MSU TLT dataset is presented in Figure 2, using the nonparametric seasonal Kendall slope estimator B (top), LS (middle) and LAD (bottom) linear regression respectively.

It is clear from Figure 2 that not only the sign of the trend but also the magnitude are extremely similar among all different estimations, resulting in equivalent spatial distribution of trends. These results support the idea that the trends observed in satellite data are not significantly sensible to the fitting method. In other words, computed temperature trends from UAH MSU TLT dataset appear to be a robust feature and not the result of a statistical glitch. This result is also valid for the all other datasets used in this study (Figures not shown).

The UAH MSU TLT data show that generalized warming of the lower-middle

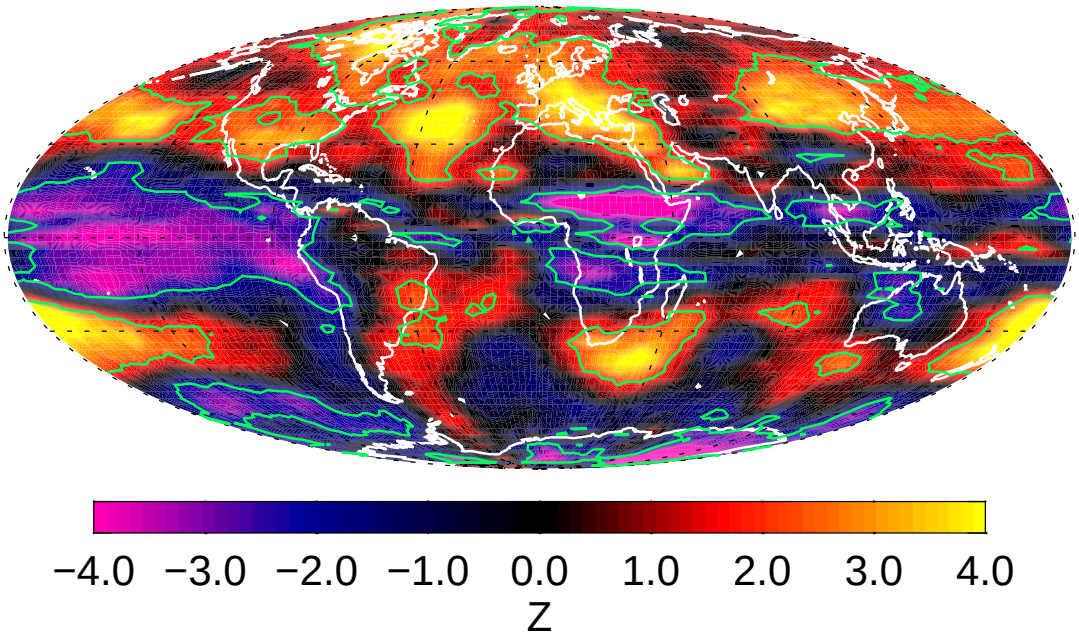

Figure 1: Spatial distribution of Z for MSU TLT. The green line represents the 95% statistical significance for randomness rejection based on Z.

troposphere is not present (see Figure 2). In fact, some regions show very consistent cooling trends, primarily over the ocean. Among these regions, the equatorial Pacific Ocean, equatorial Africa and the southern extra-tropical ocean show a statistically significant cooling trend. Other equatorial regions over South America, Atlantic Ocean and most part of Indian Ocean reveal essentially no temperature tendency. Areas with predominant warming trends are especially evident in the Northern Hemisphere above 30°N. Among these regions, Northeast Canada, Greenland, Europe and Northeast Asia present particularly large warming above 0.4 °C/Decade. An oceanic belt around 35°S from 75°E to 100°W also has a positive tendency.

MSU TLT trends are compared with the ones observed in ISCCP-TOVS dataset for the lower troposphere, available from 1983-2001. Figure 3 shows the seasonal

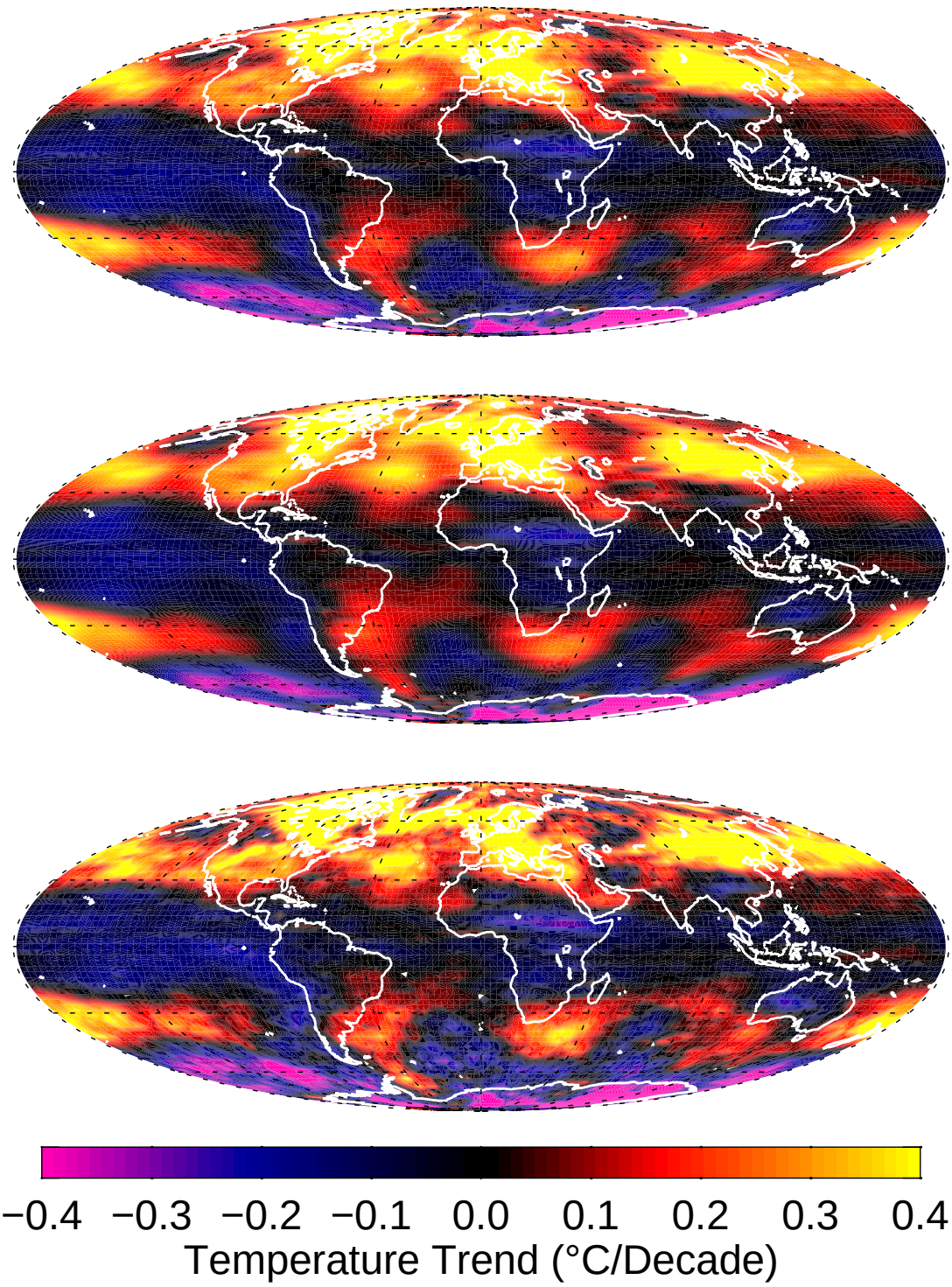

Figure 2: Estimation of the temperature trends in °C/Decade for the UAH MSU TLT dataset using the nonparametric seasonal Kendall slope estimator B (top), LS (middle) and LAD (bottom) linear regression estimators.

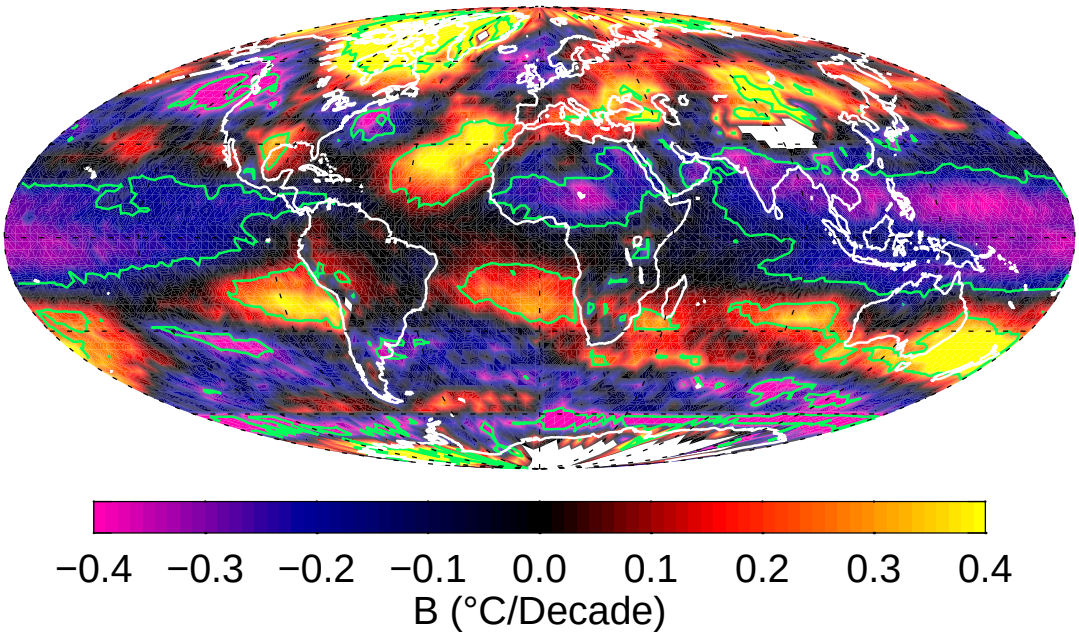

Figure 3: Distribution of nonparametric seasonal Kendall slope estimator B for ISCCP-TOVS dataset.

Kendall slope estimator B for the TOVS dataset. Although TOVS dataset has homogeneity problems, mainly due to changes in calibration over time (Dr. W. Rossow, personal communication) and the period of analysis is different, the spatial distribution of the temperature trends observed in TOVS is comparable to MSU TLT structure, with an equatorial cooling (or trendless at most), southern oceanic extratropical cooling and northern hemisphere warming being the most remarkable ones.

Although Christy et al. (2003) pointed out the difficulties for a physical interpretation of MSU TMT dataset for the mid-troposphere, since the stratosphere has some contribution to it, the spatial distribution of temperature trends, as observed in Figure 4, is very similar to the observed in MSU TLT for the low-middle troposphere but the magnitudes tend to be smaller (for both cooling and warming). The

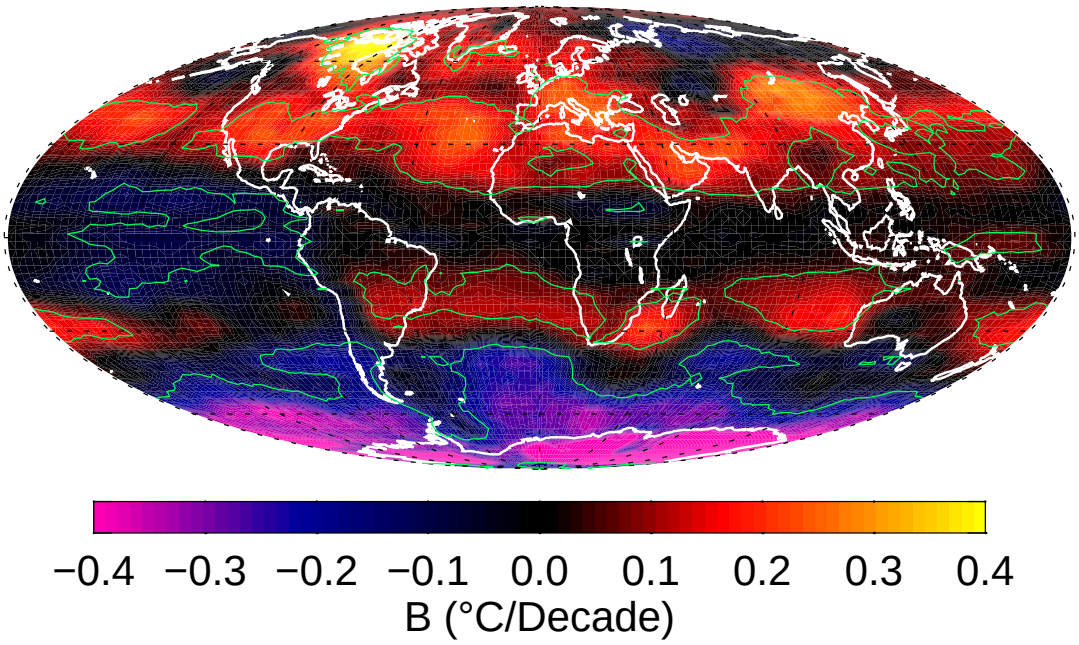

Figure 4: Distribution of nonparametric seasonal Kendall slope estimator B for UAH MSU TMT dataset.

one exception is the greater and more extensive cooling observed in the Southern hemisphere below 30°S for the middle troposphere (MSU TMT). While the Mears et al. (2003) analysis, who constructed an independent MSU dataset comparable to MSU TMT, shows substantially more warming than does the Christy et al. (Mears et al. 2003) the main spatial patterns are similar, as noted by the authors, with extratropical Southern hemisphere cooling and cooling (trendless at most) tropics.

Figure 5 shows the regional variability of temperature trends for NCEP-NCAR and ERA-40 reanalyses in layer 850-300mb. Distribution of temperature trends is comparable among both reanalyses and the MSU TLT data set. However, while the tropical cooling is present in both reanalysis, the structure in the extratropical Southern hemisphere is different, with ECMWF trends showing warming south of 50°S.

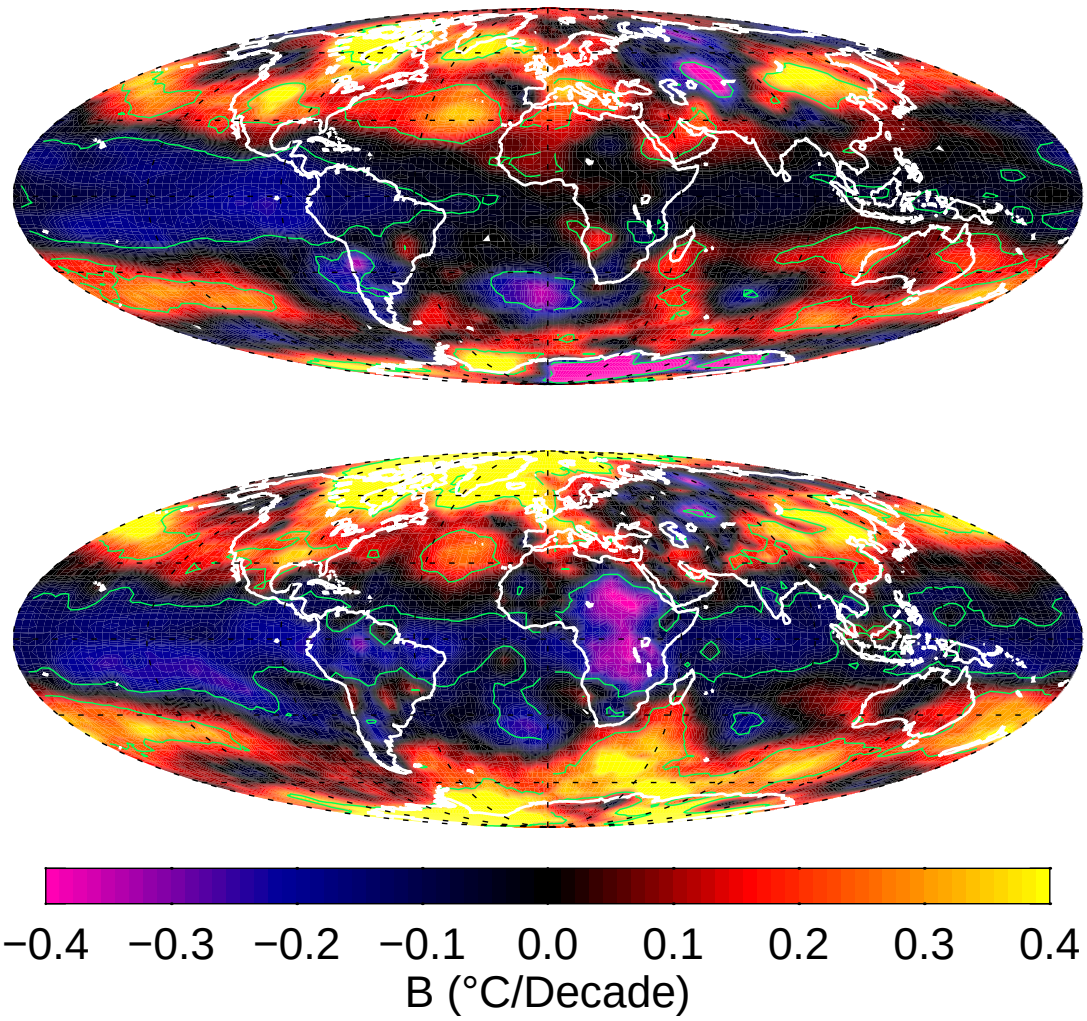

Figure 5: Nonparametric seasonal Kendall slope estimator B for NCEP-NCAR (top) and ERA-40 (bottom) reanalyses in layer 850-300mb.

Both reanalyses show Northern hemisphere warming, with the ECMWF distribution closer in magnitude to the MSU TLT. Since NCEP-NCAR trends are tied directly to radiosondes through a weekly retrieval update and ERA-40 trends are influenced by both satellite radiances and radiosondes, the reanalyses are rather independent of each other, and from the UAH MSU for long term trends.

While comparison of the different satellite analyses and NWP reanlyses generally support the UAH MSU TLT analysis in terms of regional variations, some researchers

regard the surface radiosonde network as the "gold standard" for atmospheric temperature data and long term trends. Here we examine the impact of sampling deficiencies in estimates of the global tropospheric temperature trend using radiosonde data. To address this issue, in Table 1 we collocated the MSU TLT analysis and reanalysis pixel/grid with each of 87(and 155) CARDS stations. We then calculated a "global" temperature trend for the satellite and reanalysis data sets. We further compare these trends using the CARDS locations with the true global trends derived from the satellite and reanalyses. A global estimate using 87 homogenized CARDS stations from 1979-1997 is also included. Spatial distribution of radiosonde stations can be found in Figure 6. All global, regional and collocated trend calculations were estimated by calculating the mean temperature anomalies of a specific region (or locations=cells) and then estimate the trend of the resulting time series, and not as a simple average of the trends in each cell.

In Table 1, the column "87 locations" reflects the fundamental differences among the data sets in terms of the various methods used to determine lower tropospheric temperatures. The four different trend analyses differ by a factor of 3 (about 0.08 °C/decade), with the reanalyses values intermediate to the MSU (warmest) and radiosonde (coolest). If the "global" radiosonde trend (0.044) is compared with the true global MSU trend (0.053), this apparent agreement in the radiosonde and MSU global trends masks substantial differences in the two data sets when MSU is actually co-located with the radiosondes. Comparison of the columns "87 locations"

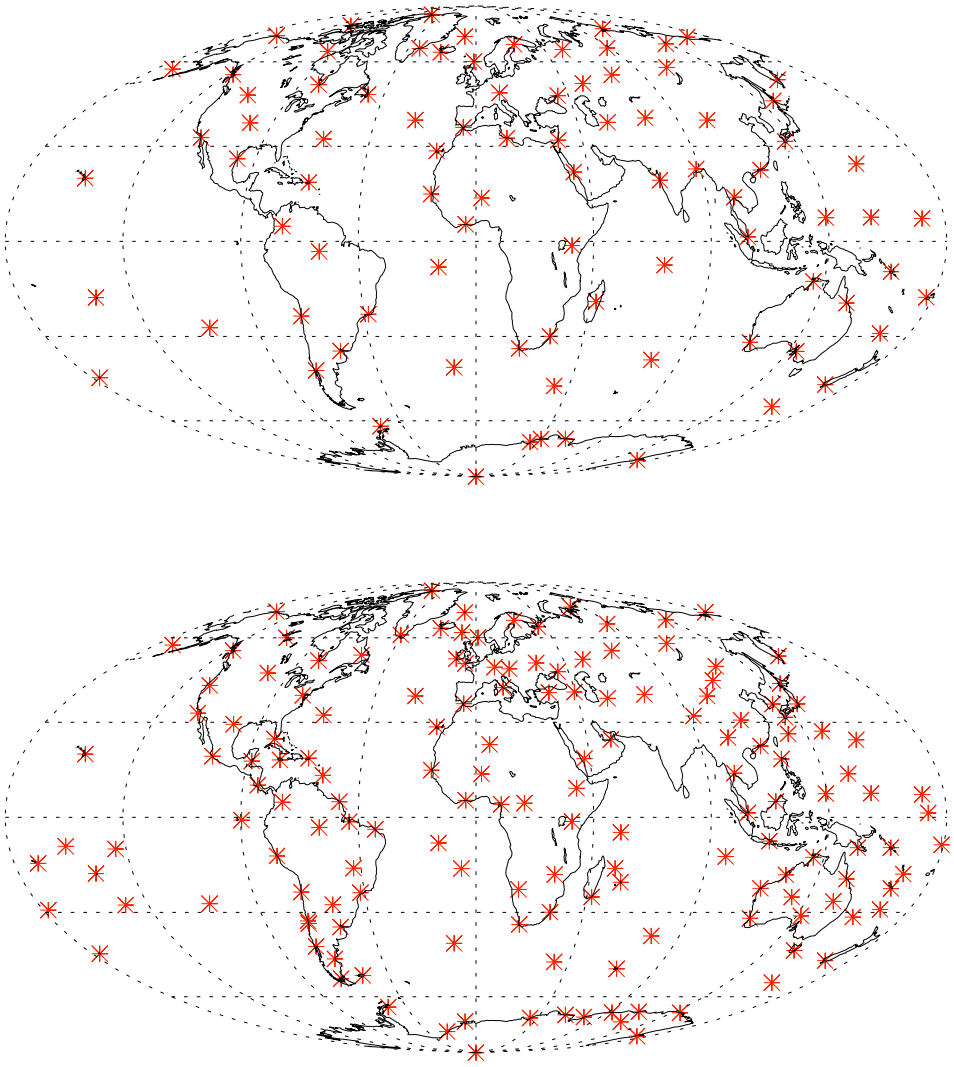

Figure 6: Spatial distribution of 87 (top) and 155 (bottom) CARDS radiosonde stations.

and "155 locations" indicates a consistent 25-30% uncertainty in the trend associated with sampling of the existing radiosonde stations to infer a "global" trend. Of particular interest is the range among MSU, NCEP-NCAR, and ECMWF of the difference in trends between "87 locations" and global, ranging from a decrease of 71% for MSU, to little change for NCEP-NCAR, to an increase of 18% for ECMWF. The dominant components of the differences between "87 locations" and global estimates

are the lack of values over the ocean and the irregular latitudinal distribution in the sounding data set.

Using the seasonal Kendall slope estimator B, the average temperature trend at the "87 locations" for the period 1979-2001 is 0.121 °C/decade as reported in the Table 1, and 0.115 °C/decade and 0.120 °C/decade using least squares and least absolute deviation estimators respectively. The similarity in the trend magnitude further confirms the existence of trends exist irrespective of the statistical tool used to detect them, as long as the time series is not very short.

In order to overcome the problem due to irregular distribution of sounding sites, so all latitudinal regions are equally important when computing a global average no matter how sparse or dense the sounding network is over different regions, different authors, including the Intergovernmental Panel on Climate Change (IPCC), have adopted a standard method, where zonal mean anomalies of those stations in a particular latitude band are computed first, and then global mean anomalies are computed from those zonal values. However, there is no clear agreement of which latitude bands should be used. If we used the latitude bands in Lanzante et al (2003) (30 to 60 in both hemispheres and -30 to 30), the global temperature trend at "87 locations" changes from 0.121 to 0.105 °C/decade, while using Angell (1988) bands (10 to 30, 30 to 60, and 60 to 90 in both hemispheres and -10 to 10), the trend is 0.081 °C/decade. We argue that the selection of latitude bands is rather subjective and does not resolve the problem. In addition, this technique does not resolve the fact that there are no measurements over the ocean.

Table 1: Seasonal Kendall slope estimator B for Global monthly temperature anomalies in the lower troposphere and the collocated "global" anomalies 1979-2001.

Data set	87 locations	155 locations	Global
MSU TLT (Christy)	0.121*	0.089*	0.053*
NCEP-NCAR (850-300)	0.049*	0.035*	0.043*
ECMWF (850-300)	0.097*	0.070*	0.119
Lanzante (850-300)$^{+}$	0.044*	-	-

+ 1979 - 1997.
$*$ values are significantly different from zero at the 95% confidence level.

To further explore the differences in the trend analyses over the oceans, we examine variations in sea surface temperature (SST). Several authors have pointed out not only that there is low correlation of anomalies between the surface and the tropospheric temperature in tropical oceanic regions but also that global tropical SST and atmospheric temperatures have shown different trends (e.g. Hurrell and Trenberth 1996, Hurrell et al. 2000, Christy et al. 2001). Here we compare the main features observed in the SST and tropospheric temperature trends. In order to estimate SST trends for the same period as the tropospheric trends (1979-2001), we combined NOAA OI-SST with GISST in the same manner as both Reanalysis projects, using GISST from 1979 to 1981 and NOAA OI-SST onwards. Since this merge could generate artificial trends (Hurrell and Trenberth, 1999), we compared the trends without the 3-GISST years and the differences in distribution and magnitude of trends are not significant. Surface temperature trends are also estimated using HadCRUT2 dataset.

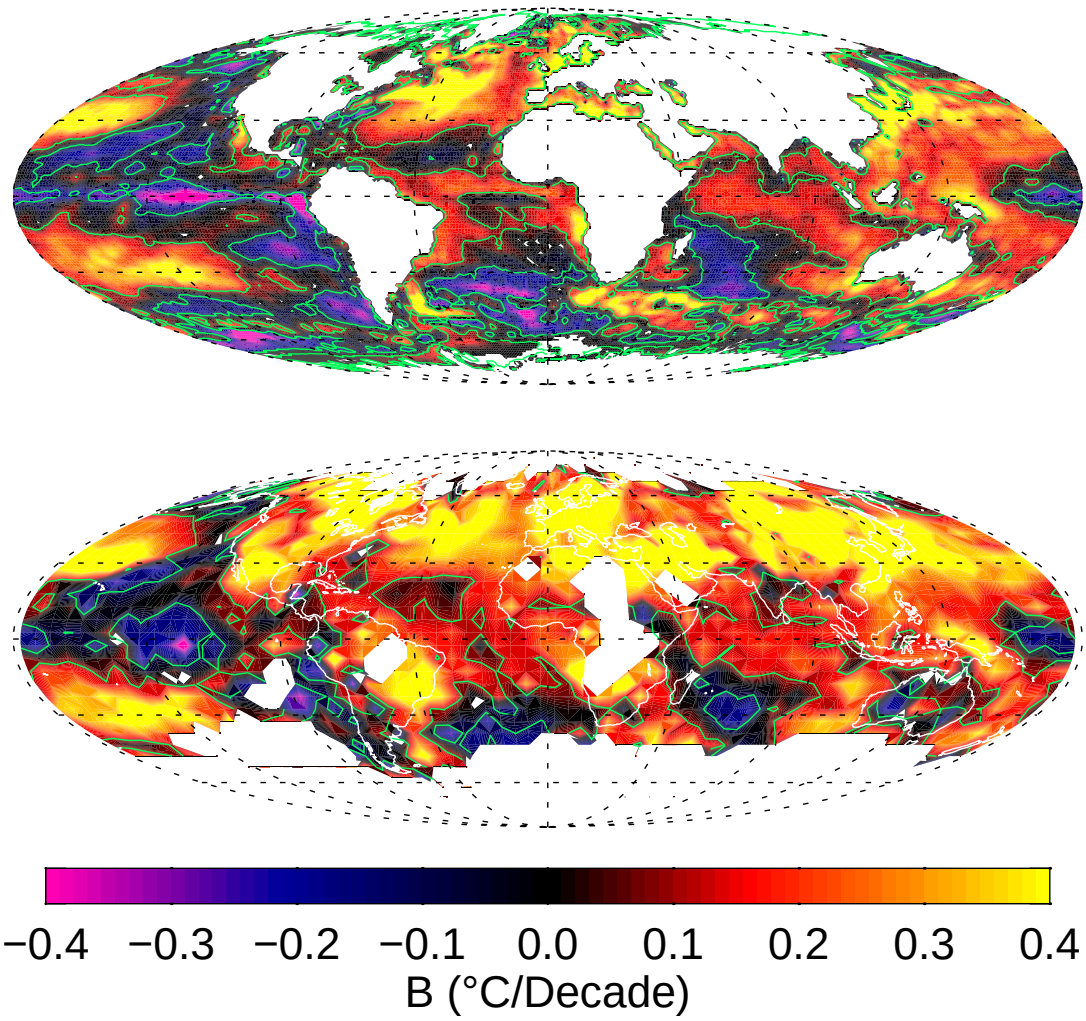

Figure 7: Nonparametric seasonal Kendall slope estimator B for NOAA OI-SST (using GISST as in Reanalysis projects) (top) and for HadCRUT2 (bottom). White areas in HadCRUT2 map correspond to those regions with more than 10% missing data in the period of the study.

Figure 7 shows the global distribution of B (°C/Decade) for the combined SST, and for the HadCRUT2 dataset. As in the case of tropospheric temperatures, it is apparent from Figure 7 that there is no generalized warming trend in the SST. Similar results are obtained using HadCRUT2. The regional variability of the SST trends shows qualitatively many of the same features shown in the MSU TLT atmospheric trends, with warming appearing predominantly in the northern hemisphere and a

Table 2: Seasonal Kendall slope estimator for the Tropics (10°S-10°N, 0-360) and two non-overlapping tropical regions (Tropics 1: 10°S-10°N, 170-280 and Tropics 2: 10°S-10°N, 290-160) from 1979 to 2001.

Dataset	Tropics	Tropics 1	Tropics 2
MSU TLT (Christy)	-0.068*	-0.118*	-0.047
NCEP-NCAR (850-300)	-0.080*	-0.145*	-0.033
ECMWF (850-300)	-0.155*	-0.166*	-0.137*
SST	0.037*	-0.114*	0.134*
HadCRUT	0.100*	-0.045	0.185*

$*$ values are significantly different than zero at the 95% confidence level.

characteristic cooling to the east of the tropical Pacific. In addition, distribution of trends for HadCRUT2 show the marked surface warming over northern hemisphere land locations. In order to contrast the observed features over the ocean and for the lower troposphere, here we compare quantitatively the trends in SST with the trends in atmospheric temperature trends for specific regions.

Over the whole tropical oceans, Christy et al. (2001) found a negative tendency for the tropospheric temperatures (MSU TLT) and a positive one for the SSTs. Table 2 compares the trends in SST and the lower troposphere for the global tropics (between 10N and 10S) and for the tropical eastern Pacific Ocean versus western Pacific Ocean and Indian Ocean. Although for the whole tropics the estimated SST trends are positive, there is a zonal gradient in the SST trends (see Figure 7). This is manifested by an overall surface cooling in the eastern tropical Pacific and warming in the western

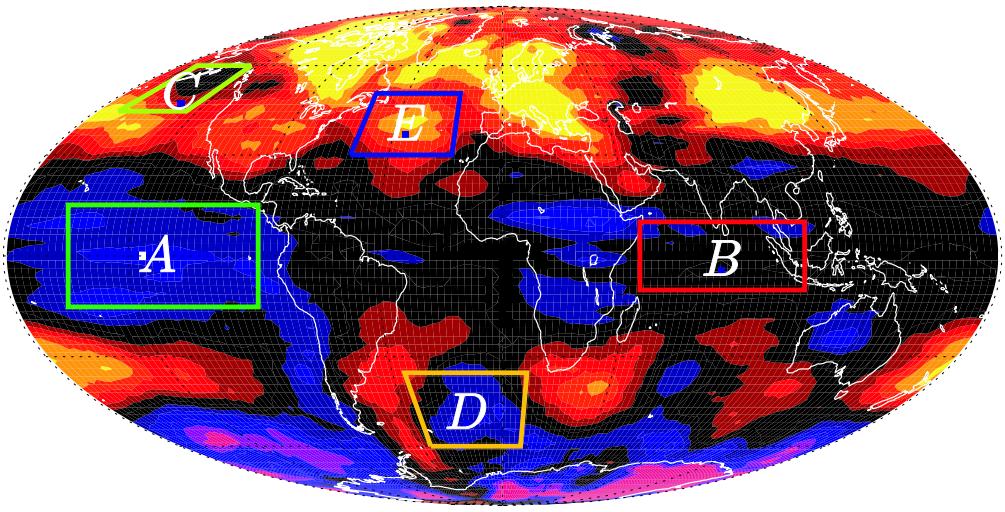

Figure 8: Localization of the regions used in Table 3 over the temperature trends for MSU TLT. Region A: 15°S-15°N, 200-270, Region B: 10°S-10°N, 50-110, Region C: 45°N-60°N, 190-220, Region D: 65°S-35°S, 320-10, Region E: 30°N-50°N, 300-340.

tropical Pacific and Indian Ocean. The atmospheric cooling trend is consistent with the cooling trend in SST over the Eastern Pacific, but opposite in sign over the Western Pacific Ocean and Indian Ocean. We note that the atmospheric temperature trends over the Western Pacific Ocean and Indian Ocean from MSU TLT and NCEP-NCAR are substantially smaller than the cooling trend observed in ECMWF ERA-40, and are not statistically different from zero.

Table 3 compares the SST and the tropospheric trends for five different regions in the global ocean. Figure 8 shows the location of the selected regions. In the tropical eastern Pacific, a cooling tendency is seen for both the surface and the atmospheric temperatures. A high correlation of the surface and atmospheric temperature anomalies in this region was noted by Hurrell and Trenberth (1996). Over the equatorial Indian Ocean (Region B) trends in SST are positive, differing in sign from the negative tropospheric temperature trends. A region including the Gulf of Alaska (Region

Table 3: Seasonal Kendall slope estimator for the period 1979-2001 for Region A: 15°S-15°N, 200-270, Region B: 10°S-10°N, 50-110, Region C: 45°N-60°N, 190-220, Region D: 65°S-35°S, 320-10, Region E: 30°N-50°N, 300-340.

Dataset	A	B	C	D	E
MSU TLT (Christy)	-0.144*	-0.047	0.046	-0.073	0.272*
NCEP-NCAR (850-300)	-0.173*	-0.031	0.030	-0.038	0.185*
ECMWF (850-300)	-0.183*	-0.091*	0.052	0.159*	0.174*
SST	-0.078*	0.126*	-0.115*	-0.111*	0.371*
HadCRUT2	-0.034	0.157*	-0.045	-0.218*	0.398*

$*$ values are significantly different than zero at the 95% confidence level.

C) shows the atmosphere with slightly positive trends and a strong cooling trend over the ocean. Region D, in the Southern Ocean, shows cooling in the SST, MSU and NCEP-NCAR, while ECMWF shows strong warming. This non-conclusive evidence could be related to the fact that quality of SST records in the Southern Ocean is questionable. Over the north Atlantic (Region E) both atmospheric and oceanic trends are significantly positive.

Such troposphere-ocean surface differences might be explained if thermal trends are considered together with regional dynamical/thermodynamical features and possible trends in the circulation, particularly in the Indian Ocean and the western tropical Pacific where the atmosphere undergoes important dynamical changes in several temporal scales. The fact that NCEP-NCAR and ERA-40 reanalyses, that use the same SST data sets used in Figure 7, are able to capture differing trends between the

ocean and the atmosphere might imply that models used for reanalysis are simulating the necessary dynamics/thermodynamics that could lead to a tropospheric cooling in contrast to a surface warming.

CHAPTER IV

CONCLUSIONS

This work has focused on regional variability in tropospheric and sea surface temperature trends during the period 1979-2001. The Christy MSU TLT analysis and the NCAR/NCEP and ECMWF reanalyses show qualitatively similar regional distributions in tropospheric temperature trends, although the magnitudes differ among the data sets. Spatial distribution of temperature trends also remained unchanged when different statistical tools, both parametric and non-parametric, where used to estimate them. All three analyses show substantial regional variability in temperature trends, with the magnitude of the variability (including substantial regions with cooling trends) far exceeding the average global warming trend. Given this large variability, inferences using the global average value can be misleading for a variety of applications.

Collocation of the MSU and reanalysis data sets with the location of the CARDS radiosonde data set showed a factor of 3 variability in the different estimates of tropospheric temperature trends. From the regional variability shown by the MSU and reanalyses, we infer that the subsampled 87 locations results in a overestimate by 25-30% of the temperature trend relative to the complete data set with 155 locations. A fortuitous (and potentially misleading) agreement between the "global" estimates using the homogenized radiosonde data set (87 locations) with the global MSU value

masks a factor of 3 difference in the collocated temperature trends.

Recent observations of sea surface temperature and tropospheric temperature showing opposite trends are clarified regionally, including documentation of a strong gradient in sea surface temperature trends in the tropical Pacific Ocean, with surface cooling in the east and warming in the west. Analysis of the reanalysis products lends credibility to the differences in signs of trends between the sea surface and tropospheric temperature trends whereby it appears that models used for reanalysis are simulating the necessary dynamics/thermodynamics that could lead to a tropospheric cooling in the presence of a surface warming (and vice versa).

While improved estimates of magnitudes of global atmospheric warming trends awaits improved analysis of the satellite data sets, we have demonstrated that the regional variability of the trends observed by satellite is qualitatively consistent with the reanalyses. While the utility of the reanalysis products has not been established for documenting global average tropospheric temperature trends, this study has demonstrated their utility in documenting and clarifying regional variability in temperature trends. Such regional analysis is necessary to understand the differences among different data sets, which is important for improved estimates of global trends as well as regional trends, the latter which may eventually be more useful for applications and policy making.

REFERENCES

[1] Angell, J. K., "Variations and trends in tropospheric and stratospheric global temperatures, 1958-87," *J. Climate*, 1, 1296-1313, 1988.

[2] Angell, J. K., "Effect of exclusion of anomalous tropical stations on temperature trends from a 63-station radiosonde network, and comparison with other analyses," *J. Climate*, 16, 2288-2295, 2003.

[3] Bengtsson, L., S. Hagemann, and K. I. Hodges, "Can climate trends be calculated from reanalysis data?," *J. Geophys. Res.*, 109, D11111, doi:10.1029/2004JD004536, 2004

[4] Christy, J.R., D.E. Parker, S.J. Brown, I. Macadam, M. Stendel and W.B. Norris, "Differential trends in tropical sea surface and atmospheric temperatures," *Geophys. Res. Lett.*, 28, 183-186, 2001.

[5] Christy, John R., R. W. Spencer, W. B. Norris, W. D. Braswell, Parker, E. David, "Error Estimates of Version 5.0 of MSU-AMSU Bulk Atmospheric Temperatures," *J. Atmos. Ocean. Tech.*, 20, 613-629, 2003.

[6] Christy, J. R., and W. B. Norris, "What may we conclude about global tropospheric temperature trends?," *Geophys. Res. Lett.*, 31, L06621, doi:10.1029/2003GL019361, 2004.

[7] Eskridge, R. E., O. A. Alduchov, I. V. Chernykh, P. Zhai, A. C. Polansky, and S. R. Doty, "A Comprehensive Aerological Reference Dataset (CARDS): Rough and Systematic errors," *Bull. Amer. Meteor. Soc.*, 76, 1759-1775, 1995.

[8] Gaffen, D.J., "Temporal inhomogeneities in radiosonde temperature records," *J. Geophys. Res.*, 99, 3667-3676, 1994

[9] Gaffen, D. J., M. A. Sargent, R. E. Habermann, and J. R. Lanzante, "Sensitivity of tropospheric and stratospheric temperature trends to radiosonde data quality," *J. Climate*, 13, 1776-1796, 2000.

[10] Hirsh, R.M., J.R, Slack, and R. Smith, "Techniques of trend analysis for monthly water quality data," *Water Resour. Res.*, 18, 107-121, 1982.

[11] Houghton, J. T., Y. Ding, D. J. Griggs, M. Noguer, P. J. Linden, X. Dai, K. Maskell, and C. A. Johnson, Eds, Climate Change 2001, "The Scientific Basis. Cambridge University Press," 881 pp, 2001.

[12] Hurrell, J. W., and K. E. Trenberth, "Satellite versus surface estimates of air temperature since 1979," *J. Climate*, 9, 2222-2232, 1996.

[13] Hurrell, J., S. Brown, K. Trenberth, and J. Christy, Comparison of the tropospheric temperatures from radiosondes and satellites: 1979-98, *Bull. Amer. Meteor. Soc.*, 81, 2165-2177, 2000

[14] Kalnay, E., et al., "The NCEP/NCAR 40-year reanalysis project," *Bull. Am. Meteor. Soc.*, 77, 437-471, 1996.

[15] Lanzante, J. R., S. A. Klein, and D. J. Seidel, "Temporal homogenization of monthly radiosonde temperature data. Part I: Methodology," *J. Climate*, 16, 224-240. 2003a

[16] Lanzante, J. R., S. A. Klein, and D. J. Seidel, "Temporal homogenization of monthly radiosonde temperature data. Part II: Trends, sensitivities, and MSU comparison," *J. Climate*, 16, 241-262, 2003b

[17] Mann, H.B., "Non-parametric tests against trend," *Econometrica*, 13, 245-259, 1945.

[18] Mears, C. A., M. C. Schabel, and F. J. Wentz, "A Reanalysis of the MSU Channel 2 Tropospheric Temperature Record," *J. Climate*, 16, 3650-3664, 2003.

[19] Molnar, P. and J.A. Ramirez, "Recent Trends in Precipitation and Streamflow in the Rio Puerco Basin," *J. Climate*, 14, 2317-2318, 2001.

[20] NRC, "Reconciling Observations of Global Temperature Change. NRC Panel on Reconciling Temperature Observations," National Academy Press, 85 pp., 2000.

[21] Prabhakara, C., J. R. Iaacovazzi, J.-M. Yoo and G. Dalu, "Global warming: Evidence from satellite observations," *Geophys. Res. Lett.*, 27, 3517-3520, 2000.

[22] Rayner, N.A., E.B. Horton, D.E. Parker, C.K. Folland, and R.B. Hackett, "Version 2.2 of the Global sea-ice and Sea Surface Temperature data set, 1903-1994," CRTN74, Hadley Centre for Climate Prediction and Research, Met. Office, 1996.

[23] Rayner, N. A., D. E. Parker, E. B. Horton, C. K. Folland, L. V. Alexander, D. P. Rowell, E. C. Kent, and A. Kaplan, "Global analyses of sea surface temperature, sea ice, and night marine air temperature since the late nineteenth century," *J. Geophys. Res.*, 108, 4407, doi:10.1029/2002JD002670, 2003.

[24] Reynolds, R. W. and T. M. Smith, "Improved global sea surface temperature analyses," *J. Climate*, 7, 929-948, 1994.

[25] Rossow, W.B., A.W. Walker, D.E. Beuschel, and M.D. Roiter, "International Satellite Cloud Climatology Project (ISCCP): Documentation of New Cloud Datasets," WMO/TD-No. 737, World Meteorological Organization, 115 pp, 1996.

[26] Santer, B. D., J. J. Hnilo, T. M. L. Wigley, J. S. Boyle, C. Doutriaux, M. Fiorino, D. E. Parker and K. E. Taylor, "Uncertainties in 'observational' estimates of temperature change in the free atmosphere," *J. Geophys. Res.*, 104, 6305-6334, 1999

[27] Santer, B. D., T. M. L. Wigley, J. S. Boyle, D. J. Gaffen, J. J. Hnilo, D. Nychka, D. E. Parker, and K. E. Taylor, "Statistical significance of trends and trend differences in layer-average atmospheric temperature time series," *J. Geophys. Res.*, 105, 7337-7356, 2000.

[28] Siedel, D. J., J. K, Angell, M. Free, J. Christy, R. Spencer, S. A. Klein, J. R. Lanzante, C. Mears, M. Schabel, F. Wentz, D. Parker, P. Thorne, and A. Sterin, "Uncertainty in signals of large-scale climate variations in radiosonde and satellite upper-air temperature datasets," *J. Climate*, 17, 2225-2240, 2004.

[29] Simmons, A. J., and J. K. Gibson, "The ERA-40 project plan," ERA-40 Project Rep. Series 1, 62 pp., 2000.